Available online at www.sciencedirect.com
ScienceDirect
Preventive Veterinary Medicine 85 (2008) 166–186
PREVENTIVE VETERINARY MEDICINE
www.elsevier.com/locate/prevetmed

Explaining Usutu virus dynamics in Austria: Model development and calibration

Franz Rubel [a,*], Katharina Brugger [a,b], Michael Hantel [b], Sonja Chvala-Mannsberger [c], Tamás Bakonyi [d,e], Herbert Weissenböck [c], Norbert Nowotny [d]

[a] *Department of Natural Sciences, University of Veterinary Medicine, Vienna (VUW), Veterinärplatz 1, A-1210 Vienna, Austria*
[b] *Institute for Meteorology and Geophysics, University of Vienna, Althanstrasse 14, A-1090 Vienna, Austria*
[c] *Department of Pathobiology, VUW, Veterinärplatz 1, A-1210 Vienna, Austria*
[d] *Department of Diagnostic Imaging, Infectious Diseases and Clinical Pathology, VUW, Veterinärplatz 1, A-1210 Vienna, Austria*
[e] *Department of Microbiology and Infectious Diseases, Faculty of Veterinary Science, Szent István University, Hungaria krt. 23-24, H-1143 Budapest, Hungary*

Received 22 May 2007; received in revised form 10 January 2008; accepted 14 January 2008

Abstract

Usutu virus (USUV), a flavivirus of the Japanese encephalitis virus complex, was for the first time detected outside Africa in the region around Vienna (Austria) in 2001 by Weissenböck et al. [Weissenböck, H., Kolodziejek, J., Url, A., Lussy, H., Rebel-Bauder, B., Nowotny, N., 2002. Emergence of Usutu virus, an African mosquito-borne flavivirus of the Japanese encephalitis virus group, central Europe. Emerg. Infect. Dis. 8, 652–656]. USUV is an arthropod-borne virus (arbovirus) circulating between arthropod vectors (mainly mosquitoes of the *Culex pipiens* complex) and avian amplification hosts. Infections of mammalian hosts or humans, as observed for the related West Nile virus (WNV), are rare. However, USUV infection leads to a high mortality in birds, especially blackbirds (*Turdus merula*), and has similar dynamics with the WNV in North America, which, amongst others, caused mortality in American robins (*Turdus migratorius*). We hypothesized that the transmission of USUV is determined by an interaction of developing proportion of the avian hosts immune and climatic factors affecting the mosquito population. This mechanism is implemented into the present model that simulates the seasonal cycles of mosquito and bird populations as well as USUV cross-infections. Observed monthly climate data are specified for the temperature-dependent development rates of the mosquitoes as well as the temperature-dependent extrinsic-incubation period. Our model reproduced the observed number of dead birds in Austria between 2001 and 2005, including the peaks in the relevant years. The high number of USUV cases in 2003 seems to

* Corresponding author. Tel.: +43 1 25077 4325; fax: +43 1 25077 4390.
E-mail address: franz.rubel@vu-wien.ac.at (F. Rubel).

0167-5877/$ – see front matter
doi:10.1016/j.prevetmed.2008.01.006

be a response to the early beginning of the extraordinary hot summer in that year. The predictions indicate that >70% of the bird population acquired immunity, but also that the percentage would drop rapidly within only a couple of years. We estimated annually averaged basic reproduction numbers between $\bar{R}_0 =$ 0.54 (2004) and 1.35 (2003). Finally, extrapolation from our model suggests that only 0.2% of the blackbirds killed by USUV were detected by the Austrian USUV monitoring program [Chvala, S., Bakonyi, T., Bukovsky, C., Meister, T., Brugger, K., Rubel, F., Nowotny, N., Weissenböck, H., 2007. Monitoring of Usutu virus activity and spread by using dead bird surveillance in Austria, 2003–2005. Vet. Microbiol. 122, 237–245]. These results suggest that the model presented is able to quantitatively describe the process of USUV dynamics.

Keywords: Infectious disease; Usutu virus; West Nile virus; SIR model; Epidemic model; Basic reproduction number; *Culex pipiens*; Climate forcing; Seasons

1. Introduction

Usutu virus (USUV), a member of the mosquito-borne clade within the Flaviviridae family (Kuno et al., 1998; Bakonyi et al., 2004) was first identified in Austria in late summer 2001 (Weissenböck et al., 2002). The virus was responsible for mortality of blackbirds (*Turdus merula*) and great grey owls (*Strix nebulosa*) in the city of Vienna and surrounding villages. USUV was originally isolated from mosquitoes in South Africa in 1959 and was named after a river in Swaziland (Woodall, 1963). USUV then was isolated sporadically from several mosquito and bird species in Africa (Odelola and Fabiyi, 1976). Only two isolations were reported from mammals: one from African solt-furred rats (*Praomys* sp.) and one from a man with fever and rash (Adam and Diguette, 2007). The virus was considered to be unimportant in terms of pathogenicity because it has never been associated with severe or fatal diseases in animals or humans. Furthermore it was never before observed outside tropical and subtropical Africa. However, following its emergence in Austria 2001, USUV has been highly pathogenic for several species of wild birds (especially blackbirds). The disease was characterized by encephalitis, myocardial degeneration, and necrosis in liver and spleen (Chvala et al., 2004). A complete genome analysis of the Austrian USUV compared to the South African reference strain SAAR-1776 found 97% nucleotide and 99% amino-acid identity (Bakonyi et al., 2004). In 2002–2005, the virus continued to kill birds in eastern Austria. The detection of USUV in mosquitoes showed that USUV had managed to overwinter and had been able to establish an efficient local bird–mosquito transmission cycle. In the years 2003–2005 a dead-bird surveillance system was established to study the further development of USUV activity (Chvala et al., 2007). The most remarkable trends were a peak of viral activity in late summer 2003 (resulting in considerable blackbird mortality) and a subsequent decline of USUV-associated bird losses in the following summers of 2004 and 2005.

USUV is closely related to West Nile virus (WNV) and the Austrian epidemic showed similarities to the recent WNV epidemic in North America. Thus, we were able to take advantage from the comprehensive work on WNV, that had been done following the introduction of WNV to the American continent in 1999. Nevertheless, there were several unanswered questions on arbovirus transmission; for example Thomas and Urena (2001) state in referring to the American WNV epidemics: *Experts are unsure what triggers an outbreak of the virus. Researchers believe a combination of climate, bird, and mosquito dynamics and other variable factors can lead to*

initial outbreaks of the virus. However, the exact combination of these factors remains a mystery. As a contribution to solve this multi-factorial problem, we demonstrate on the basis of the USUV epidemics in Austria, how the climate, bird and mosquito interaction triggers the spread of mosquito-borne diseases. We developed a model and simulated the observed USUV dynamics in Austria.

Recent epidemic models have been developed for malaria (Anderson and May, 1991), WNV (Thomas and Urena, 2001; Wonham et al., 2004; Bowman et al., 2005; Cruz-Pacheco et al., 2005) and Eastern Equine Encephalitis virus (EEEV) (Unnasch et al., 2006). All these models consider both mosquito and bird population dynamics, respectively, but with the limitation of constant parameters. On the other hand, entomologists and biometeorologists independently developed mosquito-population models, mostly formulated as life-table or matrix models, with weather-, climate- or hydrology-dependent parameters (Focks et al., 1993; Eisenberg et al., 1995; Hoshen and Morse, 2004; Ahumada et al., 2004; Ward, 2005; Shaman et al., 2006; Otero et al., 2006). We combined both these approaches and added mosquito hibernation (the ''diapause'') to simulate the spread of mosquito-borne infections in the middle and higher latitudes.

We adopted existing WNV models for USUV transmission and extended to a multi-season model driven by temperature data. Furthermore, we used a logistic (density-dependent) population growth by considering carrying capacities for both mosquitoes and birds. We herein present the first version of our model; we included a comparison to the observed bird-mortality data from the USUV monitoring program, annually averaged basic reproduction numbers $\bar{R}_0$ and some sensitivity analysis.

2. Formulation of the epidemic model

We developed an SIR type (susceptible-infected-removed) model based on two single-species (bird and mosquito) populations models. The populations are connected by the cross-infection between the species. Both single-species models simulate multi-seasonal population dynamics by considering density-dependent growth rates and seasonal temperatures.

2.1. Population models for birds and mosquitoes

The simplest possible single-species population model, here related to the population of birds and formulated by an ordinary differential equation (ODE), may be written as

$$\frac{\mathrm{d}N_\mathrm{B}}{\mathrm{d}t} = r_\mathrm{B} N_\mathrm{B} = b_\mathrm{B} N_\mathrm{B} - m_\mathrm{B} N_\mathrm{B} \tag{1}$$

wherein N_B is the total density of birds and $r_\mathrm{B} = b_\mathrm{B} - m_\mathrm{B}$ is the reproduction rate of birds, i.e. the difference between birth rate b_B and mortality rate m_B. Eq. (1) describes an exponential (unlimited) population growth, frequently applied in epidemic models (Wonham et al., 2004), but in reality observed only during shorter time periods. For the long-term dynamics, we investigated the logistic growth model (a density-dependent approach)

$$\frac{\mathrm{d}N_\mathrm{B}}{\mathrm{d}t} = r_\mathrm{B}\left(1 - \frac{N_\mathrm{B}}{K_\mathrm{B}}\right)N_\mathrm{B} = \left(b_\mathrm{B} - (b_\mathrm{B} - m_\mathrm{B})\frac{N_\mathrm{B}}{K_\mathrm{B}}\right)N_\mathrm{B} - m_\mathrm{B} N_\mathrm{B} \tag{2}$$

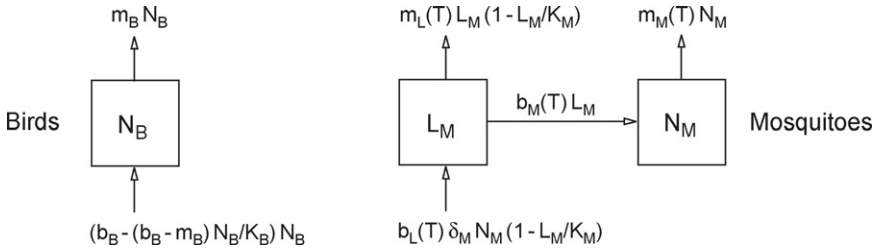

Fig. 1. Block diagram of the population models depicting the life cycles of birds (left) and mosquitoes (right).

where the carrying capacity K_B limits the bird population. K_B is the maximal density of birds carried by the environment (Fig. 1, left).

The density-dependent population model for mosquitoes is formulated in a similar way, but is based on two compartments: one for the aquatic stages of mosquitoes (eggs, larvae and pupae) and one for the terrestrial stages (the adults). Fig. 1(right) depicts the block diagram for the mosquito model where the density of the aquatic stages is named ''larvae'' L_M and the total density of adult mosquitoes is represented by N_M. The system of ODEs for the mosquito model is:

$$\frac{dL_M}{dt} = (b_L N_M - m_L L_M)\left(1 - \frac{L_M}{K_M}\right) - b_M L_M \tag{3}$$

$$\frac{dN_M}{dt} = b_M L_M - m_M N_M \tag{4}$$

The mosquito density is bounded by K_M (the carrying capacity of the mosquito larvae). K_M may, for example, account for the availability of small water bodies preferred by *Culex* mosquitoes to deposit their egg rafts.

The seasonality of the mosquito-population cycle is a consequence of the temperature-dependent birth and mortality rates. These are $b_L(T)$, the birth rate of larvae (egg-deposition rate of female mosquitoes), $m_L(T)$, the mortality rate of larvae, $b_M(T)$, the birth rate of adult mosquitoes (maturation rate, larvae to adults) and $m_M(T)$, the mortality rate of the adult mosquitoes, respectively. Only female mosquitoes take blood meals and therefore contribute to USUV transmission—so mosquito densities in the model relates only to females. Additionally, the hibernation of adult mosquitoes (diapause) is considered by δ_M, the fraction of non-diapausing mosquitoes determined by the photoperiod (see Section 3.5). Thus, the final ODEs for the mosquito population model are:

$$\frac{dL_M}{dt} = (b_L(T)\delta_M N_M - m_L(T) L_M)\left(1 - \frac{L_M}{K_M}\right) - b_M(T) L_M \tag{5}$$

$$\frac{dN_M}{dt} = b_M(T) L_M - m_M(T) N_M \tag{6}$$

This model is forced by the environmental temperature. The functions for the temperature-dependent mosquito birth and mortality rates are given in Section 3.3.

In their classical model *Daisyworld*, Watson and Lovelock (1983) investigated two plant species (black and white daisies) the abundance of which followed nonlinearly coupled ODEs

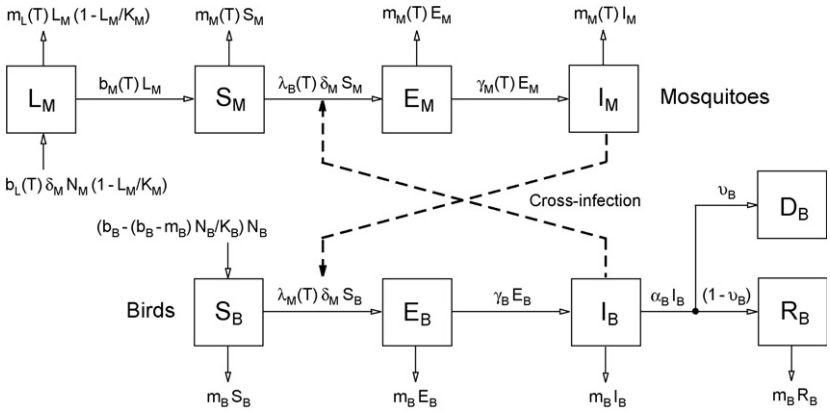

Fig. 2. Block diagram of the epidemic model depicting the life cycles of birds and mosquitoes as well as the cross-infection between these two species (dashed lines).

of the same type as Eqs. (5) and (6). The coefficients of the corresponding Daisyworld equations were also temperature-dependent, but otherwise defined differently. Thus the dynamics of the Watson and Lovelock model was quantitatively different, but qualitatively similar, to our model.

2.2. Epidemic model with cross-infection

To simulate USUV dynamics, the population models for birds (Eq. (2)) and mosquitoes (Eqs. (5) and (6)) were extended to an arbovirus model. The bird population is divided into the health states susceptible (S_B), latent infected (E_B), infectious (I_B) and removed, whereas the removed birds were separated into immune (i.e., recovered; R_B) and dead (D_B) individuals. As depicted in Fig. 2, we defined three rates for the transition from one health state to another. The first rate is λ_M (the force of infection[1]), the second rate is γ_B, the virus reproduction rate (the reciprocal of the intrinsic-incubation period), and the third rate is α_B (the removal rate). The latter is divided into death and immunization rate by ν_B, the fraction of birds dying due to an infection with the virus. Thus, $\nu_B\alpha_B$ is the death rate and $(1 - \nu_B)\alpha_B$ is the immunization rate of the birds. Note that both horizontal and vertical virus transmission in birds is neglected. The total density of birds is now $N_B = S_B + E_B + I_B + R_B$ and the dead birds D_B may be compared to the observed numbers from the USUV monitoring program (Chvala et al., 2007).

Analogously, the mosquito population was divided into the health states susceptible (S_M), latent infected (E_M) and infectious (I_M), with the total density of mosquitoes $N_M = S_M + E_M + I_M$. Unlike birds, infectious mosquitoes remain in the infectious state for the rest of their lifetime. Vertical virus transmission in mosquitoes is neglected. Again, λ_B is the force of infection and $\gamma_M(T)$ is now the reciprocal of the extrinsic-incubation period, which is a function of the environmental temperature.

[1] Incidence is defined as the product of $\lambda_M\delta_M S_B$.

The forces of infection $\lambda_B(T)$ and $\lambda_M(T)$ are defined following the concept proposed by Anderson and May (1991) and applied e.g. by Wonham et al. (2004). According to this, the cross-infection between mosquitoes and birds is modeled as mass-action kinetics normalized by the maximal density of birds K_B:

$$\lambda_B(T) = \beta_B(T)\frac{I_B}{K_B} = k(T)\ p_B\frac{I_B}{K_B} \tag{7}$$

$$\lambda_M(T) = \beta_M(T)\frac{I_M}{K_B} = k(T)\ p_M\frac{I_M}{K_B} \tag{8}$$

The terms $\beta_B(T)$ and $\beta_M(T)$ denote the transmission rate of birds and mosquitoes, respectively, and are calculated as the product of the biting (contact) rate on birds $k(T)$ and the transmission probability from birds to mosquitoes p_B or from mosquitoes to birds p_M. The contact rate $k(T)$ is the reciprocal of the gonotrophic cycle which depends on the environmental temperature (Reisen et al., 2006). Because both epidemic terms comprise mosquito densities, they are multiplied by δ_M to account for hibernation. The epidemic terms read as $\delta_M\beta_B(T)S_MI_B/K_B$ and $\delta_M\beta_M(T)I_MS_B/K_B$, respectively.

The total epidemic process discussed above and depicted by the block diagram in Fig. 2 is described by nine ODEs; these are ODEs for five health states of birds

$$\frac{dS_B}{dt} = \left(b_B - (b_B - m_B)\frac{N_B}{K_B}\right)N_B - \delta_M\beta_M(T)I_M\frac{S_B}{K_B} - m_BS_B \tag{9}$$

$$\frac{dE_B}{dt} = \delta_M\beta_M(T)I_M\frac{S_B}{K_B} - \gamma_BE_B - m_BE_B \tag{10}$$

$$\frac{dI_B}{dt} = \gamma_BE_B - \alpha_BI_B - m_BI_B \tag{11}$$

$$\frac{dR_B}{dt} = (1-\nu_B)\alpha_BI_B - m_BR_B \tag{12}$$

$$\frac{dD_B}{dt} = \nu_B\alpha_BI_B \tag{13}$$

and for four states of mosquitoes

$$\frac{dL_M}{dt} = (b_L(T)\delta_MN_M - m_L(T)L_M)\left(1 - \frac{L_M}{K_M}\right) - b_M(T)L_M \tag{14}$$

$$\frac{dS_M}{dt} = -\delta_M\beta_B(T)S_M\frac{I_B}{K_B} + b_M(T)L_M - m_M(T)S_M \tag{15}$$

$$\frac{dE_M}{dt} = \delta_M\,\beta_B(T)S_M\frac{I_B}{K_B} - \gamma_M(T)E_M - m_M(T)E_M \tag{16}$$

$$\frac{dI_M}{dt} = \gamma_M(T)E_M - m_M(T)I_M \tag{17}$$

Eqs. (9)–(17) are solved numerically and require the estimation of the model parameters, i.e. the transition rates, as well as the specification of the initial conditions.

Table 1
Model parameters: per capita rates in units days^{-1}and fractions for birds (left) and mosquitoes (right)

Parameter	Value	Interpretation	Parameter	Value	Interpretation
			b_L	$f(T)$	Birth rate, larvae
			m_L	$f(T)$	Mortality rate, larvae
b_B	$f(d)$	Birth rate, birds	b_M	$f(T)$	Birth rate, mosquitoes
m_B	0.0012	Mortality rate, birds	m_M	$f(T)$	Mortality rate, mosquitoes
α_B	0.182	Removal rate, birds			
β_B	$f(T)$	Transmission rate	β_M	$f(T)$	Transmission rate
γ_B	0.667	Rate infected-infectious, with $1/\gamma_B$ intrinsic-incubation period	γ_M	$f(T)$	Rate infected-infectious, with $1/\gamma_M$ extrinsic-incubation period
ν_B	0.3	Fraction birds dying due to infection	δ_M	$f(d, \varphi)$	Fraction mosquitoes non-diapausing

$b_B(d)$ is a function of the calendar day (Fig. 3) and $\beta_B(T)$ is a function of the temperature. The mosquito rates $b_L(T)$, $m_L(T)$, $b_M(T)$, $m_M(T)$, $\beta_M(T)$ and $\gamma_M(T)$ are functions of temperature (Figs. 4 and 5). $\delta_M(d, \varphi)$ is a function of the calendar day and the geographical latitude, respectively (Fig. 6). Typical values for $T = 25\,^\circ$ C are $\beta_B = 0.028$ days^{-1}, $b_L = 0.537$ days^{-1}, $m_L = 0.238$ days^{-1}, $b_M = 0.054$ days^{-1}, $m_M = 0.024$ days^{-1}, $\beta_M = 0.231$ days^{-1} and $\gamma_M = 0.097$ days^{-1}. Note that the model will be applied for several years ($d \neq$ const.) and observed temperatures ($T \neq$ const.).

3. Parameter estimation

The extent to which an epidemic model simulates reality depends strongly on the assumed parameters. Thus, a major part of this study concerned to the accurate estimation of the model parameters. An overview of model parameters, generally defined per capita and per day, is given in Table 1. According to this, the transmission rate of birds and all mosquito rates were defined by functions of the environmental temperature, *T*. Further, the birth rate of birds were defined by a function of the Julian calendar day, *d*, and the fraction of non-diapausing mosquitoes were defined by the Julian calendar day as well as the geographical latitude, φ. The other parameters were constants.

3.1. Bird parameters

Because >90% of all birds which died from USUV infections were blackbirds (*T. merula*), we focused this study on this species. Blackbirds are widespread in woodland, but also one of the most striking birds in urban gardens. Their average life expectancy is $\sim$2 years (in exceptional cases, >20 years). Hatchwell et al. (1996) specified annual mortality rates of $m_B = 0.34$ years^{-1} and 0.52 years^{-1} in woodland and farmland, respectively. We applied a mean mortality rate of $m_B = 0.43$ years^{-1} corresponding to $m_B = 0.0012$ days^{-1}.

In central Europe blackbirds deposit eggs two to four times per year. Schnack (1991) investigated the breeding success and clutch sizes of blackbirds in 17 city parks in Vienna and in an adjacent lowland forest. On average a clutch size of 4.1 eggs was estimated for the city of Vienna and 4.6 eggs for the woodland. The breeding success (the number of fledged nestlings per eggs laid), was 22.4% for urban blackbirds and 30.7 % for forest blackbirds. Similar results were documented by Tomialojć (1993, 1994) for blackbirds in Poland (mean clutch size of 4.5 eggs, emerging nest losses of 50–92% with mean 68%). On averaged 2.5 young per pair fledged yearly, whereas the most successful pairs reared 8–9 young (Tomialojć, 1994). We assume 2.5 young per pair as bird birth rate. This yields a per capita birth rate of $b_B = 1.25$ years^{-1}or 0.00342 days^{-1}.

Although the mortality rate is assumed to be uniformly distributed over the year, a seasonal cycle was fitted to the observed birth rate. Fig. 3(left) depicts the observed frequency distribution

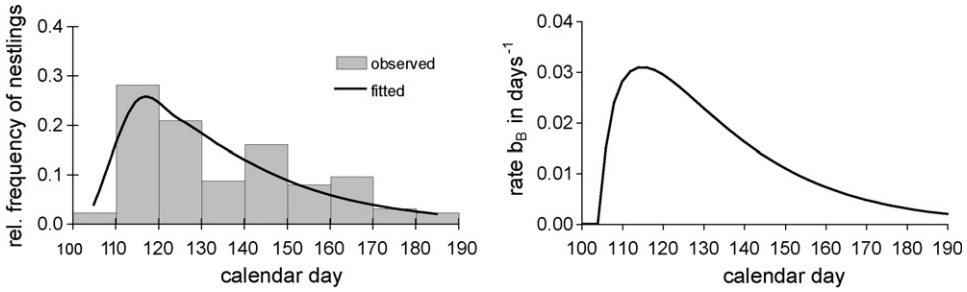

Fig. 3. Observed relative frequency of blackbird nestlings (Tomialojć, 1994) with fitted gamma distribution (left) and bird birth rate as function of the Julian calendar day (right).

of the blackbird nestlings (bars), as compiled from counts of blackbird clutches in Poland (Tomialojć, 1994), and the fitted theoretical distribution (line). Originally, Tomialojć (1994) published absolute numbers of clutches for two observational periods, which were averaged and shifted by 10 days to account for breeding. As depicted in Fig. 3(left), the distribution is skewed to the right. Therefore, a gamma distribution was selected to describe the observations. By multiplying it with the average annual birth rate $b_B = 1.25$ years^{-1}, the distribution of the birth rate as a function of the calendar day, d, is calculated as follows:

$$b_B = \frac{1.25}{10} \frac{(x/\beta)^{\alpha-1} \exp(-x/\beta)}{\beta \Gamma(\alpha)}, \quad x, \alpha, \beta > 0 \tag{18}$$

where the fraction 1/10 considers for the class width and $x = (d - 105)/10$ is the transformed Julian calendar day. The parameters of the gamma distribution were determined as $\alpha = 1.52$ and $\beta = 1.93$. Finally, the value of the gamma function is $\Gamma(\alpha) = 0.887$, as tabulated in common statistic books. The birth rate b_B as calculated with Eq. (18) is depicted in Fig. 3(right).

The breeding density in the city of Vienna varies in the range of 10–210 pairs/km^2(Schnack, 1991), corresponding to a bird density of 20–420 birds/km^2. Two typical blackbird habitats outside the city of Vienna were investigated by Wichmann and Zuna-Kratky (1997). The first habitat is an area covered with vineyards and fallow lands, and the bird density was 77–122 birds/km^2. The second habitat, a mixed forest with embedded grasslands, showed a slightly higher bird density of 104–155 birds/km^2. These densities are much higher than the large-scale blackbird density for central Europe, for example, of 25 birds/km^{2}as estimated for the entire region of Germany (Schwarz and Flade, 1989). Considering both the large-scale density and the local densities of favored blackbird habitats, we assumed an average blackbird density for the area of USUV emergence of ~ 50 birds/km^2. We used this value to scale the model by the carrying capacity of the birds K_B.

An accurate estimation of the bird mortality due to USUV infections is difficult. From the data of the dead-bird surveillance we estimated that ~ 30 % ($\nu_B = 0.3$) of the infected blackbirds died (Weissenböck et al., 2002).

3.2. Temperature-dependent transmission parameters

As for WNV, *Culex* mosquitoes are mainly responsible for USUV transmission. On average these mosquitoes are biting every 1–5 days, corresponding to biting rates of $k = 0.2$–1 days^{-1} (see for example the overview given by Cruz-Pacheco et al. (2005)). Temporal changes in the effectiveness of transmission essentially delineate the seasonality of WNV and USUV activity

and are triggered by the environmental temperature. For a description of this process, the temperature dependence of the duration of the gonotrophic cycle (i.e. the development cycle of mosquitoes comprising blood meal as well as development and deposition of eggs) as presented by Reisen et al. (2006) was used. The following function was fitted to the reciprocal of the duration of the mosquito gonotrophic cycle, and describes the biting (i.e. contact) rate:

$$k(T) = \frac{0.344}{1 + 1.231\exp\left(-0.184(T - 20)\right)}, \tag{19}$$

where T is the temperature in degree Celsius. As described in Section 2.2, the transmission rates are calculated as the product of the contact rate and the transmission probabilities: $\beta_B(T) = k(T)\,p_B$ and $\beta_M(T) = k(T)\,p_M$. Typical WNV probabilities p_B and p_M as proposed by various authors were summarised by Wonham et al. (2004) and vary in the range of $p_B = 0.02 - 0.24$ and $p_M = 0.8 - 1.0$. We determined the transmission probabilities by fitting the model to observations (see Section 5).

3.3. Temperature-dependent mosquito parameters

The temperature dependence of mosquito birth and mortality rates (of both larvae and adult mosquitoes) were investigated mainly in the 1960s and 1970s. Unfortunately, most of these studies do not provide functions as required for process models. Therefore, one of our goals was to find general functions describing the relationship between mosquito population parameters and environmental temperature. A selection of functions fitted to data sets published by various authors is depicted in Fig. 4.

Fig. 4 a shows the birth rate of larvae $b_L(T)$, a synonym for the egg-deposition rate, which is modeled by the scaled reciprocal of the gonotrophic cycle after Reisen et al. (2006). We selected the scaling factor (see Eq. (20)) so that the average birth rate $b_L(T) = 0.537\ \text{days}^{-1}$, as proposed by Wonham et al. (2004), is reached at $T = 25\,^{\circ}\text{C}$. Typical mortality rates of larvae are shown in Fig. 4 b, where a function was fitted to data from Bailey and Gieke (1968). Alternative functions (not shown) were used for example by Eisenberg et al. (1995) or Shaman et al. (2006). Most studies are available for the temperature-dependent birth rate of adult mosquitoes $b_M(T)$ (that is, the development rate of immatures). These studies comprise laboratory experiments for *C* ulex quinquefasciatus and *Aedes aegypti* (Rueda et al., 1990), a regression line for *Culex annulirostis* (Rae, 1990) as well as discrete values for *Culex tarsalis* (Reisen, 1995) and for *Culex pipiens molestus* (Olejnícek and Gelbic, 2000). Logistic functions $b_M(T)$ were fitted to all of these data sets and subsequently were evaluated in sensitivity studies (results not presented). As an example, the function fitted to the data published by Reisen (1995) is shown in Fig. 4 c. Finally, Fig. 4 d shows the mortality rate $m_M(T)$, again as fitted to observations from Reisen (1995).

From inspection of Fig. 4, it became clear that that the functions for the population parameters of the mosquito larvae are of similar shape, but about one order of magnitude higher than those for the adult mosquitoes. Using this allowed us to generalize the mosquito birth and mortality rates. For the birth rates the following logistic (S-shaped) function was selected for application:

$$b_L(T) = 2.325\,k(T) \tag{20}$$

$$b_M(T) = \frac{b_L(T)}{10} \tag{21}$$

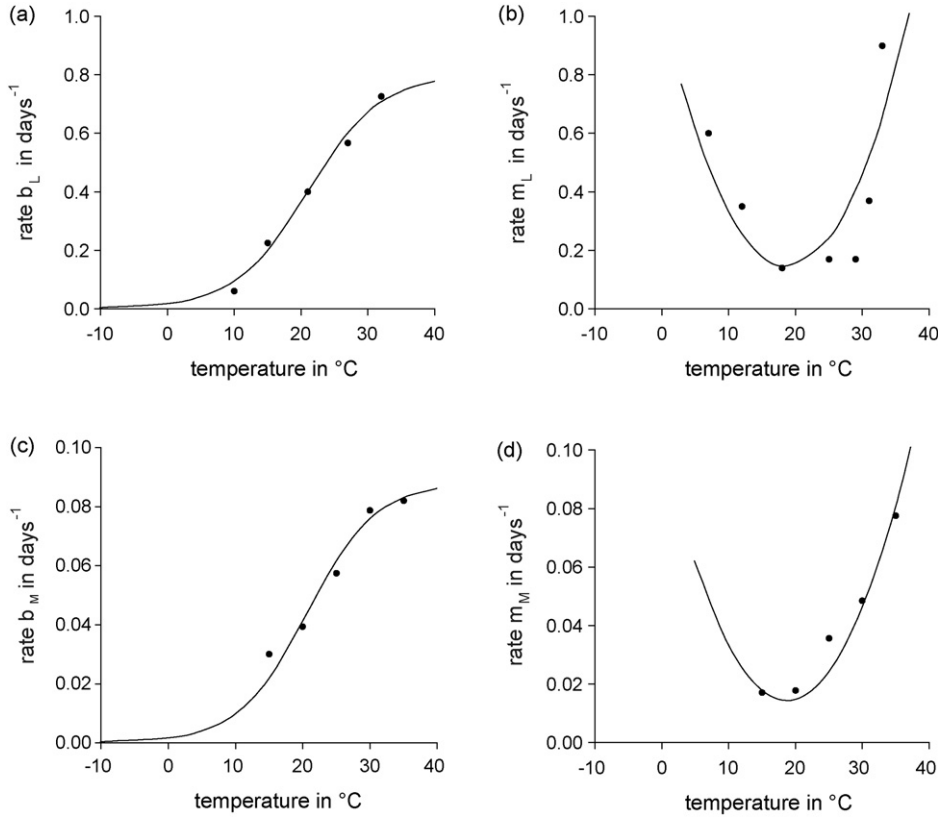

Fig. 4. Observed mosquito birth and mortality rates as function of temperature. (a) Function $b_{\mathrm{L}}(T)$ fitted to data from Reisen et al. (2006) and adjusted according to Eq. (20). (b) Function $m_{\mathrm{L}}(T)$ fitted to data from Bailey and Gieke (1968). (c) Function $b_{\mathrm{M}}(T)$ fitted to data from Reisen (1995). (d) Function $m_{\mathrm{M}}(T)$ fitted to data from Reisen (1995). Note, that parameters for larvae are about one order of magnitude higher than for adult mosquitoes.

Again, only one U-shaped function was selected to describe both mortality rates (Fig. 4 b and d), which reads as

$$m_{\mathrm{L}}(T) = 0.0025T^2 - 0.094T + 1.0257 \tag{22}$$

$$m_{\mathrm{M}}(T) = \frac{m_{\mathrm{L}}(T)}{10} \tag{23}$$

3.4. Temperature-dependent extrinsic-incubation period

The extrinsic-incubation period (i.e. the time from an infectious blood meal until the mosquito can transmit an acquired arbovirus infection), is an important parameter determining the vector capacity. It is the reciprocal of the rate of virus replication within an infected mosquito vector; the rate is temperature-dependent (Cornel et al., 1993; Turell et al., 2002; Dohm et al., 2002; Reisen et al., 2006).

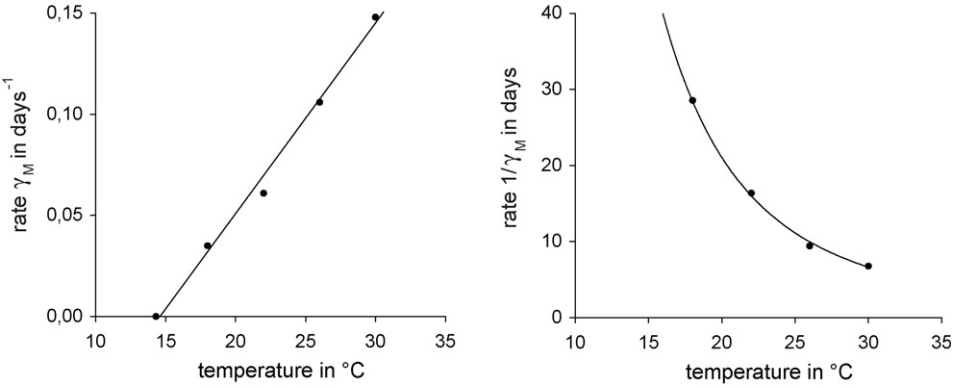

Fig. 5. Observed virus-reproduction rates (left) and its reciprocal, the extrinsic-incubation period (right), as function of temperature (fitted to data by Reisen et al. (2006)).

Because the virus-replication rate for USUV is unknown, we relied on the results from WNV. We used data from Reisen et al. (2006) to fit the functions depicted in Fig. 5. The function for the virus-reproduction rate is:

$$\begin{aligned} \gamma_M(T) &= 0.0093T - 0.1352 \quad \text{for } T > 15\,^\circ\text{C} \\ \gamma_M(T) &= 0 \qquad\qquad\qquad\quad \text{for } T \leq 15\,^\circ\text{C} \end{aligned} \tag{24}$$

Thus, the extrinsic-incubation period decreases with increasing temperature. Long periods of warm temperatures amplify flavivirus transmission. Vice versa, low temperatures can reduce the flavivirus transmission or even interrupt it when the extrinsic-incubation period exceeds the mosquito life time.

3.5. Diapause (hibernation of mosquitoes)

Quantitative investigations on the diapause of *Culex* mosquitoes are rare because they had not played an important role as vector until the 1999 WNV outbreak in New York (USA). One study was published by Eldridge (1968), who depicted the proportion of non-diapausing mosquitoes as a function of photoperiod (daytime length) and temperature (Vinogradova, 2000). A second paper was presented by Spielman (2001), who re-analyzed 50-year-old-mosquito data from Boston (300 km north of the WNV outbreak in New York) to deduce a relationship between diapause and photoperiod (dots in Fig. 6, left).

We fitted functions to both data sets: a two-dimensional function (not shown) to the data of Eldridge (1968) and a one-dimensional function to the data of Spielman (2001). Simulations demonstrated that their application yielded similar model results. This is not astonishing because of the natural correlation between the annual temperature cycle and the photoperiod. We applied the simpler relationship after Spielman (2001). This logistic function for the description of the fraction of active mosquitoes δ_M, i.e. the non-diapausing mosquitoes, reads as:

$$\delta_M = 1 - \frac{1}{1 + 1775.7 \exp\left[1.559\,(D - 18.177)\right]} \tag{25}$$

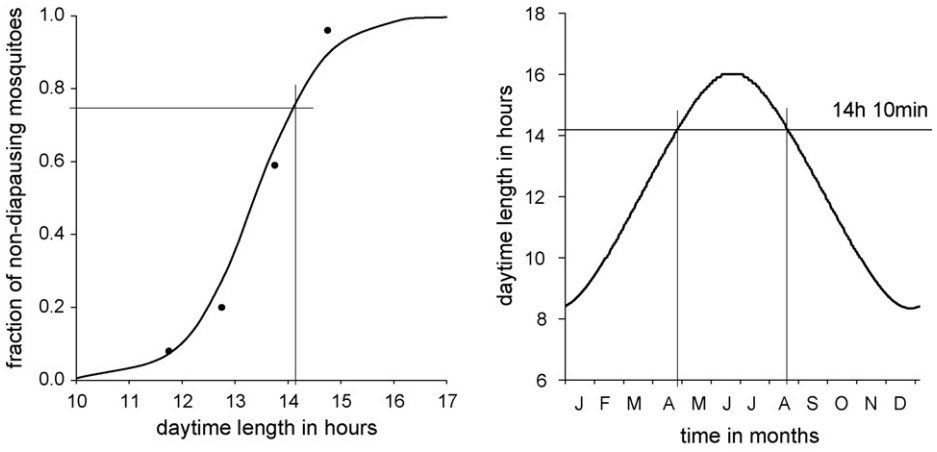

Fig. 6. Observed fraction of diapausing *Culex pipiens* mosquitoes as function of the daytime length after Spielman (2001) with fitted function (left) and annual cycle of the daytime length in hours for the geographical latitude of Vienna, Austria (right). At daytime lengths above 14 h and 10 min (May–August) >75 % of the mosquitoes are active.

and is depicted in Fig. 6(left). D is the daytime length in hours, which depends on the declination[2] ϵ and the geographic latitude φ.

$$D = 7.639 \arcsin\left[\tan(\epsilon)\tan(\varphi) + \frac{0.0146}{\cos(\epsilon)\cos(\varphi)}\right] + 12 \tag{26}$$

The annual cycle of D is depicted in Fig. 6(right). For the calculation of D the declination ϵ is required, which can be calculated for each calendar day d from the following astronomical equation:

$$\epsilon = 0.409 \sin\left(\frac{2\pi(d - 80)}{365}\right) \tag{27}$$

Thus, the fraction of non-diapausing mosquitoes as a function of the daytime length is well-defined by the geographical latitude and the calendar day.

4. Basic reproduction number

The basic reproduction number R_0 is a key parameter in the study of an infection because it sets the threshold for its establishment ($R_0 > 1$) or its extinction ($R_0 < 1$). We calculated the basic reproduction number from the dominant eigenvalue of the next-generation operator as described by Diekmann and Heesterbeek (2000) and applied to WNV models by Wonham et al. (2006).

In a infection-free equilibrium (IFE), the bird equilibrium is defined as $(S_B, E_B, I_B, R_B, D_B) = (S_B^*, 0, 0, 0, 0)$ and the mosquito equilibrium is defined as $(L_M, S_M, E_M, I_M) = (L_M^*, S_M^*, 0, 0)$, with S_B^*, L_M^* and S_M^* as the numbers of birds, larvae and mosquitoes at IFE. We rewrote the equations with infection terms (Eqs. (10), (11), (16) and (17)) in terms of the difference between

[2] In astronomy, declination is one of the two coordinates of the equatorial coordinate system.

f_i, the rate of appearance of new infection in compartment i (new-infection terms), and v_i, the transfer rate of individuals into and out of compartment i (vital dynamics terms).

$$\frac{\mathrm{d}}{\mathrm{d}t}\begin{bmatrix} E_\mathrm{B} \\ I_\mathrm{B} \\ E_\mathrm{M} \\ I_\mathrm{M} \end{bmatrix} = f - v = \begin{bmatrix} \delta_\mathrm{M}\beta_\mathrm{M} I_\mathrm{M} S_\mathrm{B}/K_\mathrm{B} \\ 0 \\ \delta_\mathrm{M}\beta_\mathrm{B} I_\mathrm{B} S_\mathrm{M}/K_\mathrm{B} \\ 0 \end{bmatrix} - \begin{bmatrix} \gamma_\mathrm{B} E_\mathrm{B} + m_\mathrm{B} E_\mathrm{B} \\ -\gamma_\mathrm{B} E_\mathrm{B} + \alpha_\mathrm{B} I_\mathrm{B} + m_\mathrm{B} I_\mathrm{B} \\ \gamma_\mathrm{M} E_\mathrm{M} + m_\mathrm{M} E_\mathrm{M} \\ -\gamma_\mathrm{M} E_\mathrm{M} + m_\mathrm{M} I_\mathrm{M} \end{bmatrix} \tag{28}$$

The linearization of this reduced system about the IFE is described by the corresponding Jacobian matrices **F** and **V**:

$$\mathbf{F} = \begin{pmatrix} 0 & 0 & 0 & \delta_\mathrm{M}\beta_\mathrm{M} S_\mathrm{B}^*/K_\mathrm{B} \\ 0 & 0 & 0 & 0 \\ 0 & \delta_\mathrm{M}\beta_\mathrm{B} S_\mathrm{M}^*/K_\mathrm{B} & 0 & 0 \\ 0 & 0 & 0 & 0 \end{pmatrix} \tag{29}$$

$$\mathbf{V} = \begin{pmatrix} \gamma_\mathrm{B} + m_\mathrm{B} & 0 & 0 & 0 \\ -\gamma_\mathrm{B} & \alpha_\mathrm{B} + m_\mathrm{B} & 0 & 0 \\ 0 & 0 & \gamma_\mathrm{M} + m_\mathrm{M} & 0 \\ 0 & 0 & -\gamma_\mathrm{M} & m_\mathrm{M} \end{pmatrix} \tag{30}$$

Finally, the basic reproduction number R_0 is given as the dominant eigenvalue of $\mathbf{FV}^{-1}$ (Diekmann and Heesterbeek, 2000):

$$R_0 = \sqrt{\left[\frac{\delta_\mathrm{M}\gamma_\mathrm{M}(T)\beta_\mathrm{M}(T)}{(\gamma_\mathrm{M}(T) + m_\mathrm{M}(T))m_\mathrm{M}(T)} \frac{S_\mathrm{B}^*}{K_\mathrm{B}}\right]\left[\frac{\delta_\mathrm{M}\gamma_\mathrm{B}\beta_\mathrm{B}(T)}{(\gamma_\mathrm{B} + m_\mathrm{B})(\alpha_\mathrm{B} + m_\mathrm{B})} \frac{S_\mathrm{M}^*}{K_\mathrm{B}}\right]} \tag{31}$$

For the assumption of a constant environmental temperature, the steady-state conditions for birds and mosquitoes are simply $S_\mathrm{B}^* = K_\mathrm{B}$ and $S_\mathrm{M}^* = K_\mathrm{M}$. Thus, in Eq. (31), the term $S_\mathrm{B}^*/K_\mathrm{B} = 1$ and the term $S_\mathrm{M}^*/K_\mathrm{B} = K_\mathrm{M}/K_\mathrm{B}$. Assuming further that all mosquitoes are active ($\delta_\mathrm{M} = 1$) and $T = 25\,^\circ$ C we calculated a basic reproduction number of $R_0 = 10.85$ (parameters are given in Table 2). R_0 is defined as the number of secondary infections that result from the introduction of a single infectious individual into an entirely susceptible population.

Table 2
Model initial conditions, carrying capacities and transmission probabilities for birds (left) and mosquitoes (right)

Parameter	Value	Interpretation	Parameter	Value	Interpretation
			$L_{\mathrm{M},0}$	0.001	Larvae mosquitoes
$S_{\mathrm{B},0}$	1.0	Susceptible birds	$S_{\mathrm{M},0}$	5.0	Susceptible mosquitoes
$E_{\mathrm{B},0}$	0.0	Latent infected birds	$E_{\mathrm{M},0}$	0.0	Latent infected mosquitoes
$I_{\mathrm{B},0}$	0.0	Infectious birds	$I_{\mathrm{M},0}$	0.01	Infectious mosquitoes
$R_{\mathrm{B},0}$	0.0	Recovered birds			
$D_{\mathrm{B},0}$	0.0	Dead birds			
K_B	1.0	Carrying capacity	K_M	100.0	Carrying capacity
			$N_{\mathrm{M,min}}$	1.0	Total mosquitoes threshold for minimum
p_B	0.125	Probability of virus transmission by infectious birds	p_M	1.000	Probability of virus transmission by infectious mosquitoes

The interpretation of the previous example is suitable only for sensitivity analysis and is not possible for seasonal infections, because the number of secondary infections depends on the time of the year in which the infectious individual is introduced. In our application the seasonal infections are determined by the seasonal cycle of the measured temperatures. Especially the mosquito population, even in the absence of the infectious agent, depends on temperature (Eqs. (5) and (6)). In this case we define $S^*_M = N_M$, where N_M is the effective size of the mosquito population which is mostly significantly lower than K_M (see the simulation results in Fig. 9). Moreover, the process of virus transmission is discontinued during winter time where temperatures are too low for virus replication and mosquitoes are in hibernation. Thus, Eq. (31) needs to be solved numerically for each model time step. Averaging this basic reproduction numbers over 1 year gives $\bar{R}_0$ which may be interpreted as follows: $\bar{R}_0$ is the average number of secondary infections arising from the introduction of a single infected individual into a completely susceptible population at a random time of the year (Grassly and Fraser, 2006).

5. Climate forcing

As discussed above, the epidemic model is forced by temperature data, which determine the contact rate $k(T)$ as well as the mosquito parameters $b_L(T)$, $m_L(T)$, $b_M(T)$, $m_M(T)$ and $\gamma_M(T)$.

The air-temperature measurements from the automatic weather station located at the University of Veterinary Medicine, Vienna, were used. These measurements are available for the period 1997 to present and are representative for the study area around Vienna. The temporal resolution of the measurements is 10 min, providing the opportunity to run the epidemic model with time steps corresponding to this resolution.

On the other hand, the numbers of dead birds collected during the USUV monitoring program (Chvala et al., 2007) are only representative on a weekly or (better) monthly time scale. Our goal was to reproduce and explain the observed multi-seasonal dynamics of USUV infections. Therefore, to account for the resolution of the observations, the model was forced by monthly averaged temperature data. Nevertheless, to assure numerical stability, the model must run with time steps of 1 day or less. We used spline functions to interpolate the monthly data to the model time step. In fact, smoothed data were used to force the model. Fig. 7 (upper panel) depicts the time series of the temperature observations in Vienna for the study period 2001–2005, whereas the gray line represents the daily and the dark line the monthly averaged (smoothed) temperature. Fig. 7(lower panel) points out the temperature anomaly: the deviation from the 10-year mean 1997–2006. Conspicuously positive temperature deviations during the mosquito-activity period were observed for May–July 2002 and for May–September 2003, whereas no longer periods of extraordinary high temperatures were observed during the other years. Subject to the temperature dependence of mosquito parameters discussed in the previous section, high USUV activities were expected for 2002 and 2003. Most interesting is the year 2003, where the June–August temperatures exceed the long-term mean by >3 °C (Schönwiese et al., 2004).

6. Numerical implementation

The arbovirus model was implemented in Fortran 90, a standard computer language for mathematical applications. Further, to discretize the ODE system (Eqs. (9)–(14)), a 4th order Runge-Kutta method with a time step of 1 day was implemented. The combination of the Runge-Kutta method with daily time steps assure the convergence of solutions of the numerical approximation.

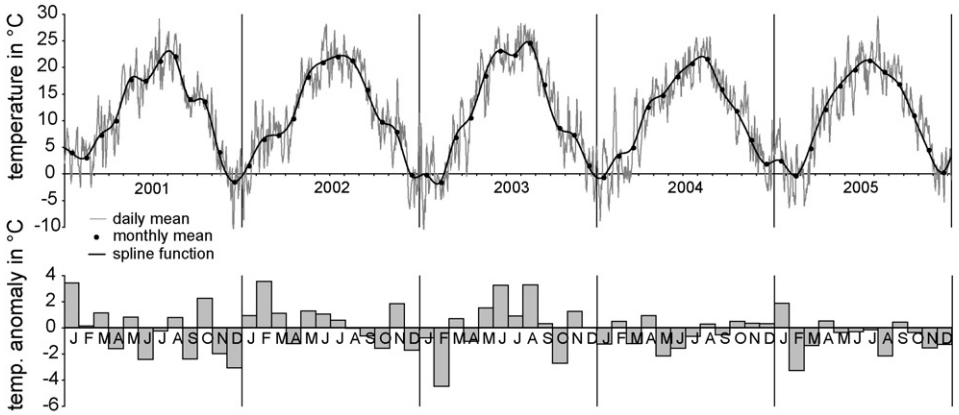

Fig. 7. Observed daily and monthly averaged temperatures (upper panel) and monthly temperature anomalies (lower panel) in degree Celsius. Location Vienna, period 2001–2005.

For practical reasons, the model was implemented with normalized health states of birds and mosquitoes, respectively. The health states were normalized with the maximal number of birds K_B, i.e. related to 1 bird, as also proposed by Wonham et al. (2004). This approach has the advantage that, at the moment, it is not necessary to know the size of both the bird population and the investigation area. For that purpose the normalized carrying capacity of the birds is defined as $K_B = 1$ bird and the normalized carrying capacity of the mosquitoes is defined as $K_M = 100$ mosquitoes (the latter may be compared to the ratio of mosquito pupae to humans necessary for dengue transmission, which was estimated by Focks et al. (2000) to range between 0.3 and >60).

By choosing the initial conditions in a way that a low number of infectious mosquitoes ($I_M = 0.01$) is introduced in a fully susceptible bird population ($N_B = S_B = 1$ and $I_B = E_B = R_B = D_B = 0$), in principle the model may run. Actually, running the temperature-forced model for several years can lead to increasing or decreasing mosquito populations, depending on the environmental temperature during winter. To avoid this numerical stability problem, a threshold for the minimal number of mosquitoes surviving the hibernation of $N_{M,min} = 1$ was assumed. This equals 1% of the maximal number of mosquitoes K_M or a proportion of $\sim 10\%$ of mosquitoes surviving hibernation, as estimated during field studies (Reiter, 2002; Medlock, 2003). Thus, the modeled mosquito population starts each season with the same initial number of mosquitoes and the USUV transmission depends only on temperatures during spring to autumn.

Before the model may be applied to simulate scenarios a final adjustment of the model parameters has to be done. As discussed in Section 3, most parameters are functions of temperature, daytime length or were taken from literature. Besides these relatively well-known parameters, the probabilities p_B and p_M, determining the forces of infection, are relatively uncertain. Therefore, optimal values for the latter were estimated by comparing the time series of simulated and observed dead birds. Fig. 8 depicts the model root mean square error (RMSE) as function of p_B and p_M. The minimum RMSE was estimated for $p_B = 0.125$ (only 12.5% of mosquito-bird contacts of an infectious bird leads to an infection of a mosquito) and $p_M = 1.00$ (nearly every mosquito-bird contact of an infectious mosquito leads to an infection of a bird), whereas the normalized model output was scaled with the so-called *observed carrying capacity*

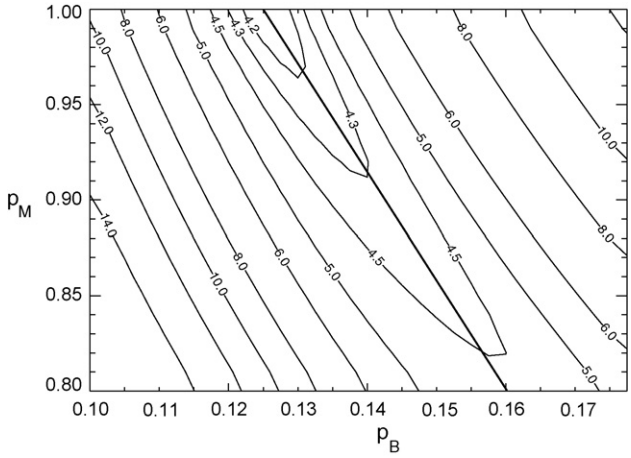

Fig. 8. Model root mean square error (RMSE), in units of dead birds, as function of p_B and p_M. The bold line depicts the minimal RMSE for the considered range of p_B and p_M.

of birds, $K_{B,obs} = 385$ birds (rounded). Further, the heavier solid line in Fig. 8, depicting the functional relationship for the minimum RMSE,

$$p_M = -5.714\, p_B + 1.714 \tag{32}$$

was used to investigate the model sensitivity to p_B and p_M. According to this, the probability parameters, estimated to be optimal for USUV transmission in Vienna, may also be selected in the range proposed by Wonham et al. (2004) for WNV ($p_B = 0.02 - 0.24$, $p_M = 0.8 - 1.0$). As long as Eq. (32) is satisfied, the model sensitivity to p_B and p_M is low. Additionally, Eq. (32) reduces the number of free parameters by one, making it simpler to calibrate the model.

The values we used for the initial conditions, the carrying capacities and the fitted transmission probabilities p_B and p_M, respectively, are summarized in Table 2.

7. Results

The first results of the model simulations were time series of health states of birds and mosquitoes. Fig. 9 (upper panel) depicts the normalized numbers of mosquito larvae and adult mosquitoes for the investigation period 2001–2005. While the mosquito population during the years 2001, 2004 and 2005 seemed typical, it was two to three times higher in 2002 and 2003. The latter were caused by the long warm periods in these years (Fig. 7). The normalized number of infectious mosquitoes, I_M (Fig. 9, lower panel) was influenced by the extrinsic-incubation period—which decreases with increasing temperature (Fig. 5).

Eq. (31) with $S_B^* = K_B$ and $S_M^* = N_M$ was used to calculate the annually averaged basic reproduction numbers $\bar{R}_0$. We calculated values of $\bar{R}_0 = 0.66$ for 2001, 1.06 for 2002, 1.35 for 2003, 0.54 for 2004, and 0.71 for 2005. Note that the condition $\bar{R}_0 < 1$ is not sufficient to prevent a USUV outbreak, since chains of transmission can be established during the high season, but is sufficient and necessary for long-term disease extinction (Grassly and Fraser, 2006).

Fig. 10 (upper panel) depicts the proportion of birds in the health states susceptible S_B, immune R_B, as well as the total population N_B. A strong increase of the immune birds $R_B \sim 0.7$ (70%) was simulated for 2003 in correspondence to the epidemic peak in the same year.

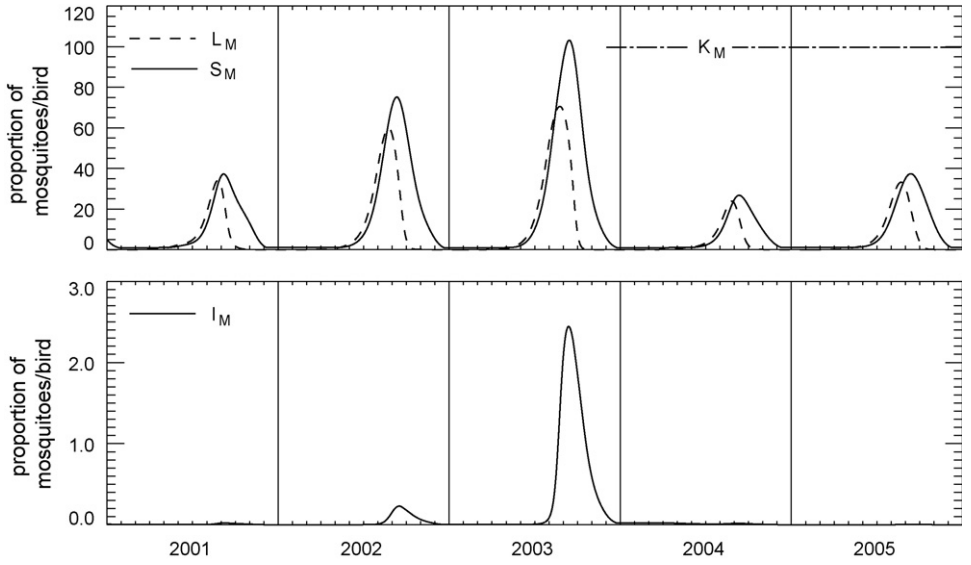

Fig. 9. Simulated time series of mosquitoes for the period 2001–2005 (proportion of mosquitoes/bird related to K_B). Upper panel: Larvae L_M (dotted line) and susceptible mosquitoes S_M (solid line) for carrying capacities $K_B = 1$ and $K_M = 100$. Lower panel: Infectious mosquitoes I_M.

Subsequently, R_B decreases to 45% until the end of 2004 and to 30% until the end of 2005. The blackbird population was not dramatically influenced by the USUV epidemics, as it has also been confirmed by observations (Loupal, G., 2006. Songbird monitoring by Bird Life Austria, personal communication). Analogous to the illustration of the time series of mosquitoes, Fig. 10(lower panel) depicts the proportion of infectious birds with the same epidemic peak in 2003.

For a comparison of simulations with observations (Fig. 11), it is necessary to scale the normalized model results. Therefore, the carrying capacity of birds, in the normalized mode assumed to be $K_B = 1$, was determined to be of order of $K_{B,obs} = 385$ by minimizing the RMSE as discussed above. Our model described the observations quite well. Note that the dead-bird monitoring was organized only for the summer months June–August, while the model simulates continuously in time. Feasible comparisons may therefore only be done for the three summer months. Nevertheless, the model simulations indicate that blackbirds die from USUV during the whole mosquito activity period May–October. Based on the estimated blackbird density of 50 birds/km^2 (see Section 3.1) and an investigation area around Vienna of ~ 3500 km^2, the true carrying capacity of blackbirds is about $K_{B,true} = 175{,}000$ birds. From the fraction $K_{B,obs}/K_{B,true}$ it follows that only 0.2% of the USUV positive birds were detected by the dead-bird monitoring program.

8. Discussion

After the epidemic peak, >70 % of the bird population acquired immunity. However, the immunity decreases very quickly and already some years after the epidemic peak in 2003 a new major outbreak can occur, depending only on the environmental temperature. Other environmental parameters such as precipitation or flooding seem to play only a minor role

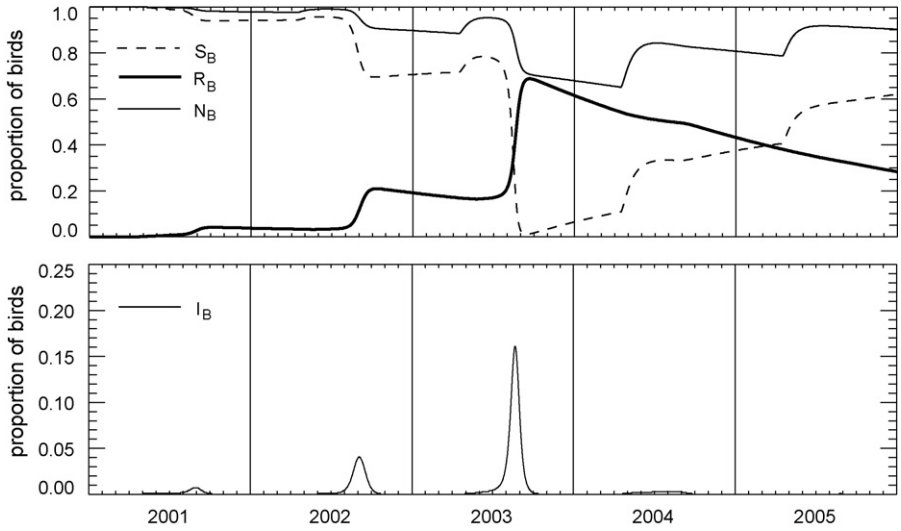

Fig. 10. Simulated time series of blackbirds for the period 2001–2005 (proportion of birds related to K_B). Upper panel: Susceptible birds S_B (dotted line), immune birds R_B (bold solid line) and total birds N_B (thin solid line) for $K_B = 1$. Lower panel: Infectious birds I_B.

(because our model fitted well without them). The 100-year flood in Vienna in August 2002, for example, had no effect on the USUV epidemics. Similar observations were made in the USA in connection with the hurricane Katrina and WNV (Farnon, 2005). The so-called flood-water mosquitoes are minor effective vectors for WNV and USUV.

A recent paper clearly demonstrated that the percentage of seropositive birds increased rapidly within the wild bird population in an endemic area—which supported the assumption that the proportion immune played a major role in the decline of USUV-associated deaths (Meister et al.,

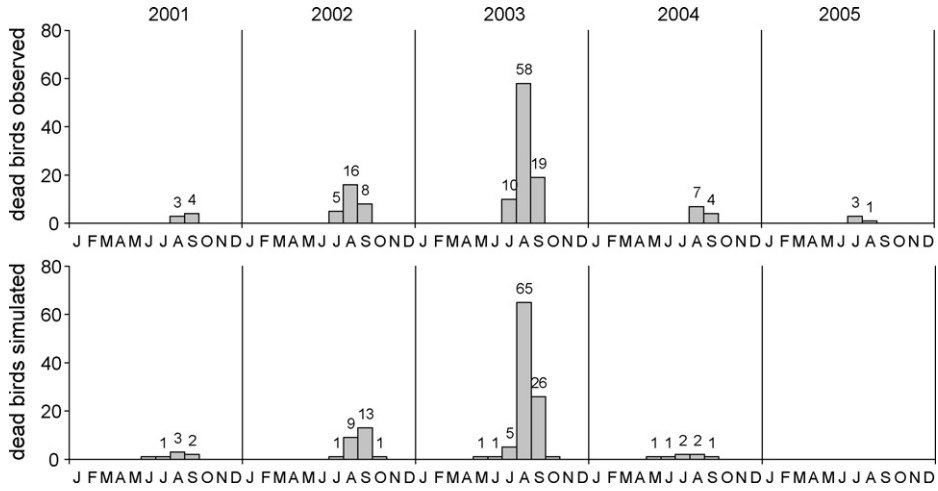

Fig. 11. Time series of monthly averaged dead blackbirds for the period 2001–2005. Upper panel: Observed. Lower panel: Simulated by the epidemic model (scaled with $K_{B,obs} = 385$). Note that the number of dead birds modeled for 2005 is below 1, but non-zero.

2008). We did not consider either vertical transmission of USUV in the mosquito vectors or horizontal transmission in susceptible birds. This decision was made because there exist no data at all on these particular transmission scenarios in USUV infections. In addition, these modes of transmission have been experimentally shown in infections with the related WNV, but their relevance in field infections seems negligible (Baqar et al., 1993; Komar et al., 2003).

A comprehensive verification of the arbovirus model might be realized in a few years when longer time series of observations are available. Especially, the population dynamics of mosquitoes of the *Culex pipiens* complex have to be verified. Unfortunately, there are no current entomological field studies in Austria. Also, the assumption that the extrinsic-incubation period of USUV (which has never been investigated in laboratory experiments) is similar to that of the closely related WNV has to be verified.

Nevertheless, our model explains the USUV transmission by combining both the effect of the immunity status of the bird population and effects of the environmental temperature. Additionally, the parameter estimation was confirmed by preliminary results of a Bayes analysis (Reiczigel et al., 2007). Thus, we propose the application of the model presented here for studies on WNV transmission in North America.

Acknowledgements

Parts of this work were funded by the *Hochschuljubiläumsstiftung der Stadt Wien* (H-1122/2006). Contributions from Katharina Brugger were supported by the research grant F130-N of the University of Vienna. A couple of points raised by the anonymous reviewer helped to improve the paper.

References

Adam, F., Diguette, J.P., 2007. Virus d'Afrique, base de donnes (in French), Centre collaborateur OMS de référence et de recherche pour les arbovirus et les virus de fiévres hémorrhagiques (CRORA). Institut Pasteur de Dakar. Available at http://www.pasteur.fr/recherche/banques/CRORA.

Ahumada, J.A., Lapointe, D., Samuel, M.D., 2004. Modeling the population dynamics of *Culex quinquefasciatus* (Diptera: Culicidae), along an elevational gradient in Hawaii. J. Med. Entomol. 41, 1157–1170.

Anderson, R.M., May, R.M., 1991. Infectious Diseases of Humans: Dynamics and Control. Oxford University Press, Oxfort, p. 757.

Bailey, S.F., Gieke, P.A., 1968. A study of the effect of water temperature on rice field mosquito development. Proc. Calif. Mosq. Vector Control Assoc. 36, 53–61.

Bakonyi, T., Gould, E.A., Kolodziejek, J., Weissenböck, H., Nowotny, N., 2004. Complete genome analysis and molecular characterization of Usutu virus that emerged in Austria in 2001: comparison with the South African strain SAAR-1776 and other flaviviruses. Virology 328, 301–310.

Baqar, S., Hayes, C.G., Murphy, J.R., Watts, D.M., 1993. Vertical transmission of West Nile virus by Culex and Aedes species mosquitoes. Am. J. Trop. Med. Hyg. 48, 757–762.

Bowman, C., Gumel, A.B., van den Driessche, P., Wu, J., Zhu, H., 2005. A mathematical model for assessing control strategies against West Nile virus. Bull. Math. Biol. 67, 1107–1133.

Chvala, S., Bakonyi, T., Bukovsky, C., Meister, T., Brugger, K., Rubel, F., Nowotny, N., Weissenböck, H., 2007. Monitoring of Usutu virus activity and spread by using dead bird surveillance in Austria, 2003–2005. Vet. Microbiol. 122, 237–245.

Chvala, S., Kolodziejek, J., Nowotny, N., Weissenböck, H., 2004. Pathology and viral distribution in fatal Usutu virus infections of birds from the 2001 and 2002 outbreaks in Austria. J. Comp. Path. 131, 176–185.

Cornel, A.J., Jupp, P.G., Blackburne, N.K., 1993. Environmental-temperature on the vector compedence of *Culex univittatus* (Diptera, Culiciade) for West Nile virus. J. Med. Entomol. 30, 449–456.

Cruz-Pacheco, G., Esteva, L., Montaño-Hirose, J.A., Vargas, C., 2005. Modelling the dynamics of West Nile Virus. Bull. Math. Biol. 67, 1157–1172.

Diekmann, O., Heesterbeek, J.A.P., 2000. Mathematical Epidemiology of Infectious Diseases. Wiley, Chichester, 303 pp.
Dohm, D.J., O'Guinn, M.L., Turell, M.J., 2002. Effect of environmental temperature on the ability of *Culex pipiens* (Diptera: Culicidae) to transmit West Nile virus. J. Med. Entomol. 39, 221–225.
Eisenberg, J.N., Reisen, W.K., Spear, R.C., 1995. Dynamic model comparing the bionomics of two isolated *Culex tarsalis* (Diptera: Culicidae) populations: model development. J. Med. Entomol. 32, 83–97.
Eldridge, B.F., 1968. The effect of temperature and photoperiod on blood-feeding and ovarian development in mosquitoes of *Culex pipiens* complex. Am. J. Trop. Med. Hyg. 17, 133–140.
Farnon, E.C., 2006. Summary of West Nile virus activity, United States 2005. In: 7th National Conference on West Nile Virus in the U.S., San Francisco, California, February 23–24. Available at http://www.cdc.gov/ncidod/dvbid/westnile/conf/February_2006.htm.
Focks, D.A., Brenner, R.D., Hayes, J., Daniels, E., 2000. Transmission thresholds for dengue in terms of *Aedes aegypti* pupae per person with discussion of their utility in source reduction efforts. Am. J. Trop. Med. Hyg. 62, 11–18.
Focks, D.A., Haile, D.G., Daniels, E., Mount, G.A., 1993. Dynamic life table model for *Aedes aegypti* (L.) (Diptera: Culicidae). Analysis of the literature and model development. J. Med. Entomol. 30, 1003–1017.
Grassly, N.C., Fraser, C., 2006. Seasonal infectious disease epidemiology. Proc. R. Soc. B 273, 2541–2550.
Hatchwell, B.J., Chamberlain, D.E., Perris, C.M., 1996. The demography of blackbirds *Turdus merula* in rural habitats: Is farmland a sub-optimal habitat? J. Appl. Ecol. 33, 1114–1124.
Hoshen, M.B., Morse, A.P., 2004. A weather-driven model of malaria transmission. Malaria J. 30, 14.
Komar, N., Langevin, S., Hinten, S., Nemeth, N., Edwards, E., Hettler, D., Davis, B., Bowen, R., Bunning, M., 2003. Experimental infection of North American birds with the New York 1999 strain of West Nile virus. Emerg. Infect. Dis. 9, 311–322.
Kuno, G., Chang, G.J., Tsuchiya, K.R., Karabatsos, N., Cropp, C.B., 1998. Phylogeny of the genus Flavivirus. J. Virol. 72, 73–83.
Medlock, J., 2003. Vector borne disease risk assessment in the UK. Available at http://www.northwest-zoonoses.info/pages/j_medlock_part2.pdf.
Meister, T., Lussy, H., Bakonyi, T., Šikutová, S., Rudolf, I., Vogl, W., Winkler, H., Frey, H., Hubálek, Z., Nowotny, N., Weissenböck, H., 2008. Serological evidence of continuing high Usutu virus (Flaviviridae) activity and establishment of herd immunity in wild birds in Austria. Vet. Microbiol. 127, 237–248.
Odelola, H.A., Fabiyi, A., 1976. Antigenic relationships among Nigerian strains of West Nile virus by complement fixation and agar gel precipitation techniques. Trans. R. Soc. Trop. Med. Hyg. 70, 138–144.
Olejnícek, J., Gelbic, I., 2000. Differences in response to temperature and sensity between two strains of the mosquito, *Culex pipiens molestu* Forskal. J. Vector Ecol. 25, 136–145.
Otero, M., Solari, H.G., Schweigmann, N., 2006. A stochastic population dynamics model for *Aedes aegypti*: formulation and application to a city with temperate climate. Bull. Math. Biol. 68, 1945–1974.
Rae, D.J., 1990. Survival and development of the immature stages of *Culex annulirostis* (Diptera: Culicidae) at the Ross River Dam in tropical eastern Australia. J. Med. Entomol. 27, 756–762.
Reiczigel, J., Brugger, K., Rubel, F., 2007. Bayes-analysis of a dynamical model for Usutu virus epidemics. In: International Conference of the German Veterinary Society, Munich, Germany, September 5–7, 2007. Available at http://i115srv.vu-wien.ac.at/staff/rubel/pdf/DVG_2007_3.pdf.
Reisen, W.K., 1995. Effect of temperature on *Culex tarsalis* (Diptera: Culicidae) from the Coachella and San Joaquin valleys of California. J. Med. Entomol. 32, 636–645.
Reisen, W.K., Fang, Y., Martinez, V.M., 2006. Effects of temperature on the transmission of West Nile virus by *Culex tarsalis* (Diptera: Culicidae). J. Med. Entomol. 43, 309–317.
Reiter, P., 2002. Biology and control of *Culex pipiens* and *Culex restuans* in Massachusetts. Studies in the Cambridge rainforest. In: 3rd National Planning Meeting for the Surveillance, Prevention, and Control of West Nile Virus in the U.S., Atlanta, Georgia, March 22–23. Available at http://www.cdc.gov/ncidod/dvbid/westnile/conf/pdf/p1-reiter.pdf.
Rueda, L.M., Patel, K.J., Axtell, R.C., Stinner, R.E., 1990. Temperature-dependent development and survival rates of *Culex quinquefasciatus* and *Aedes aegypti* (Diptera: Culicidae). J. Med. Entomol. 27, 892–898.
Schnack, S., 1991. The breeding ecology and nestling diet of Blackbird *Turdus merula* L. and Song Thrush Turdus philomelos C.L. Brehm in Vienna and adjancent wood. Acta Ornithol. 26, 85–106.
Schönwiese, C.-D., Staeger, T., Trömel, S., 2004. The hot summer 2003 in Germany. Some preliminary results of a statistical time series analysis. Meteorol. Z. 13, 323–327.
Schwarz, J., Flade, M., 1989. Ergebnisse des DDA-Monitoringprogramms Teil I: Bestandsänderungen von Vogelarten der Siedlungen seit 1989 (in German). Vogelwelt 121, 87–106.
Shaman, J.M., Spiegelman, M., Cane, M., Stieglitz, M., 2006. A hydrologically driven model of swamp water mosquito population dynamics. Ecol. Mod. 194, 395–404.

Spielman, A., 2001. Structure and seasonality of nearctic *Culex pipiens* populations. Ann. N. Y. Acad. Sci. 951, 220–234.

Thomas, D.M., Urena, B., 2001. A model describing the evolution of West Nile-like encephalitis in New York City. Math. Comp. Mod. 34, 771–781.

Tomialojć, L., 1993. Breeding ecology of blackbird *Turdus merula* studied in the primaeval forest of Bialowieza (Poland). Part 1. Breeding numbers, distribution and nest sites. Acta Ornithol. 27, 131–157.

Tomialojć, L., 1994. Breeding ecology of blackbird *Turdus merula* studied in the primaeval forest of Bialowieza (Poland). Part 2. Reproduction and mortality. Acta Ornithol. 29, 101–121.

Turell, M.J., Sardelis, M.R., O'Guinn, M.L., Dohm, D.J., 2002. Potential vectors for West Nile virus in North America. Curr. Top. Microbiol. Immunol. 267, 241–252.

Unnasch, R.S., Sprenger, T., Katholi, C.R., Cupp, E.W., Hill, G.E., Unnasch, T.R., 2006. A dynamic transmission model of eastern equine encephalitis virus. Ecol. Mod. 192, 425–440.

Vinogradova, E.B., 2000. *Culex pipiens* Pipiens Mosquitoes. Pensoft, Sofia-Moscow, p. 250.

Ward, M.P., 2005. Epidemic West Nile virus encephalomyelitis: a temperature-dependent, spatial model of disease dynamics. Prev. Vet. Med. 71, 253–264.

Watson, A.J., Lovelock, J.E., 1983. Biological homeostasis of the global environment: the parable of Daisyworld. Tellus 35B, 284–289.

Weissenböck, H., Kolodziejek, J., Url, A., Lussy, H., Rebel-Bauder, B., Nowotny, N., 2002. Emergence of Usutu virus, an African mosquito-borne flavivirus of the Japanese encephalitis virus group, central Europe. Emerg. Infect. Dis. 8, 652–656.

Wichmann, G., Zuna-Kratky, T., 1997. Monitoring von Wald- und Kulturlandschafts-Vögeln an zwei Probeflächen bei Wien-Kalksburg (in German). A study of Bird Life Austria, p. 85. Available at http://www.magwien.gv.at/umweltschutz/pool/pdf/kalksburg.pdf.

Wonham, M.J., de-Camino-Beck, T., Lewis, M.A., 2004. An epidemiological model for West Nile virus: invasion analysis and control applications. Proc. R. Soc. Lond. B 271, 501–507.

Wonham, M.J., Lewis, M.A., Renclawowicz, J., van den Driessche, P., 2006. Transmission assumptions generate conflicting predictions in host-vector disease models: a case study in West Nile virus. Ecol. Lett. 9, 706–725.

Woodall, J.P., 1963. The viruses isolated from arthropods at the East African Virus Research Institute in the 26 years ending December. Proc. E. Afr. Acad. 2, 141–146.